

Activation of the Carbon–Sulfur Bonds in Benzothiophenes by Precoordination of Transition Metals to the Carbocyclic Ring

Conor A. Dullaghan, Xiao Zhang, David L. Greene, Gene B. Carpenter, and Dwight A. Sweigart*

Department of Chemistry, Brown University, Providence, Rhode Island 02912

Chiara Camiletti

Dipartimento di Chimica Fisica e Inorganica, Viale Risorgimento 4, Bologna 40126, Italy

Edward Rajaseelan

Department of Chemistry, Millersville University, Millersville, Pennsylvania 17551

Received April 14, 1998

Coordination of an electrophilic transition-metal fragment, ML_n , to the carbocyclic ring of benzothiophene (BT) to form $(\eta^6\text{-BT})ML_n^{m+}$ activates a C–S bond to cleavage by the weak nucleophile $Pt(PPh_3)_3$, with concomitant insertion of $Pt(PPh_3)_2$. The rate of formation of the resulting metallathiacyclic insertion products, $\{(\eta^6\text{-BT}\cdot Pt(PPh_3)_2)ML_n^{m+}\}$, depends on the metal fragment in the order $ML_n = Ru(C_6Me_6)^{2+} > Mn(CO)_3^+ > FeCp^+, RuCp^+ \gg Cr(CO)_3$, with no reaction occurring in the absence of a ML_n activating group. All of the unsubstituted benzothiophene complexes undergo regiospecific cleavage of the olefinic C–S bond rather than the aryl C–S bond, which is likely a consequence of steric congestion that would exist if insertion had occurred at the latter site. The X-ray structures of the metallathiacycles $\{(\eta^6\text{-BT}\cdot Pt(PPh_3)_2)Mn(CO)_3^+\}$ and $\{(\eta^6\text{-BT}\cdot Pt(PPh_3)_2)FeCp^+\}$ are reported. The complexes $(\eta^5\text{-2,5-dimethylthiophene})Mn(CO)_3^+$ and $(\eta^6\text{-dibenzothiophene})Mn(CO)_3^+$ also undergo rapid C–S bond cleavage with metal insertion in the presence of $Pt(PPh_3)_3$. The results suggest that π -adsorption of a thiophenic substrate on a catalyst surface in hydrodesulfurization reactions is a viable way to facilitate C–S bond cleavage, as well as subsequent desulfurization and hydrodenolysis.

Introduction

Hydrodesulfurization (HDS) is an important industrial process whereby sulfur is removed from crude petroleum feedstocks and converted to H_2S .¹ This treatment is necessary to prevent catalyst poisoning in subsequent refinement steps and to reduce sulfur oxide emissions from the combustion of fossil fuels. Current HDS technology, which utilizes alumina-supported metal sulfides (e.g., Mo/Co) as catalysts, is adequate for the treatment of most sulfur-containing compounds. However, unsaturated heterocycles of the thiophenic type, especially substituted benzothiophenes (BTs) and dibenzothiophenes (DBTs), are resistant to desulfurization and, as a consequence, constitute much of the residual sulfur contamination in fossil fuels. For this reason there is substantial interest in the development of homogeneous models for thiophene desulfurization.²

Attachment of the thiophenic substrate to the metal catalyst or activator and subsequent cleavage of the

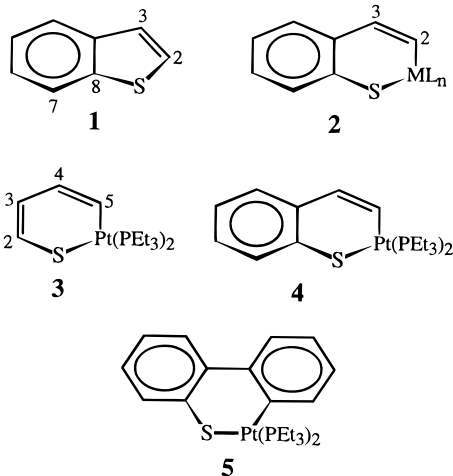
C–S bonds are two of the key steps in HDS. A number of nucleophilic 16-electron organometallic fragments are known to insert into thiophenic carbon–sulfur bonds, possibly after initial coordination to the sulfur.³ In the case of benzothiophene (BT, **1**) regiospecific metal insertion into the olefinic carbon–sulfur bond, C(2)–S, to give metallathiacycle **2** is known^{2–4} for Fe-, Ru-, Rh-, Ir-, and Pt-based fragments. The metal has never been observed to insert into the aryl carbon–sulfur bond, C(8)–S, in free unsubstituted BT. Of particular relevance to the present study is the chemistry reported

(1) (a) Sanchez-Delgado, R. A. *J. Mol. Catal.* **1994**, *86*, 287. (b) Startsev, A. N. *Catal. Rev.—Sci. Eng.* **1995**, *37*, 353. (c) Vasudevan, P. T.; Fierro, J. L. G. *Catal. Rev.—Sci. Eng.* **1996**, *38*, 161. (d) *Petroleum Chemistry and Refining*; Speight, J. G., Ed.; Taylor & Francis, Inc.: Washington, DC 1998. (e) *Hydrotreating Technology for Pollution Control*; Occelli, M. L.; Chianelli, R., Eds.; Marcel Dekker: New York, 1996.

(2) (a) Angelici, R. J. *Polyhedron* **1997**, *16*, 3073. (b) Bianchini, C.; Meli, A. *J. Chem. Soc., Dalton Trans.* **1996**, 801. (c) Bianchini, C.; Meli, A. *Acc. Chem. Res.* **1998**, *31*, 109. (d) Jones, W. D.; Vicić, D. A.; Chin, R. M.; Roache, J. H.; Myers, A. W. *Polyhedron* **1997**, *16*, 3115. (e) Stafford, P. R.; Rauchfuss, T. B.; Verma, A. K.; Wilson, S. R. *J. Organomet. Chem.* **1996**, *526*, 203.

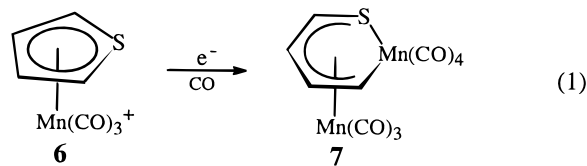
(3) (a) Dong, L.; Duckett, S. B.; Ohman, K. F.; Jones, W. D. *J. Am. Chem. Soc.* **1992**, *114*, 3328. (b) Bianchini, C.; Herrera, V.; Jimenez, M. V.; Meli, A.; Sanchez-Delgado, R.; Vizza, F. *J. Am. Chem. Soc.* **1995**, *117*, 8567.

(4) (a) Garcia, J. J.; Mann, B. E.; Adams, H.; Bailey, N. A.; Maitlis, P. M. *J. Am. Chem. Soc.* **1995**, *117*, 2179. (b) Garcia, J. J.; Arevalo, A.; Montiel, V.; Del Rio, F.; Quiroz, B.; Adams, H.; Maitlis, P. M. *Organometallics* **1997**, *16*, 3216. (c) Garcia, J. J.; Arevalo, A.; Capella, S.; Chehata, A.; Hernandez, M.; Montiel, V.; Picazo, G.; Del Rio, F.; Toscano, R. A.; Adams, H.; Maitlis, P. M. *Polyhedron* **1997**, *16*, 3185. (d) Iretskii, A.; Adams, H.; Garcia, J. J.; Picazo, G.; Maitlis, P. M. *J. Chem. Soc., Chem. Commun.* **1998**, 61.



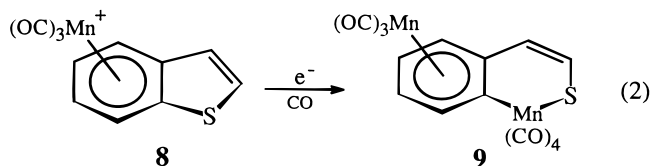
by Maitlis and co-workers,⁴ who found that Pt(PEt₃)₃ undergoes oxidative insertion into a carbon–sulfur bond in thiophene (T), BT, and DBT to afford platinum metallathiacycles **3**–**5**. Steric effects play a significant role in these reactions, as evidenced by the fact that 2,5-dimethylthiophene does not undergo the insertion reaction.

Coordination of a thiophenic molecule to a metal on an HDS catalyst surface can occur via the sulfur atom (η^1 -S bonding) or via the π -system.^{2a,5} It is easy to see that coordination to the sulfur could facilitate C–S bond scission. The effect of complexation to the π -system on the energetics of C–S cleavage is perhaps less obvious. Since HDS catalyst surfaces are multimetallic, it follows that one metal could activate the thiophenic substrate by π -coordination, making it easier for a second metal to insert into a C–S bond. Thus, Rauchfuss et al. reported⁶ that η^5 -coordination of Ru(C₆Me₆)²⁺ to thiophene activates the system to C–S cleavage upon reaction with a reducing agent and a second (electrophilic) metal. In a process that may be related mechanistically, we showed⁷ that η^5 -coordination of the Mn(CO)₃⁺ moiety to thiophene (**6**) affords the bimetallic **7** when reduced under CO (eq 1). With benzothiophene,



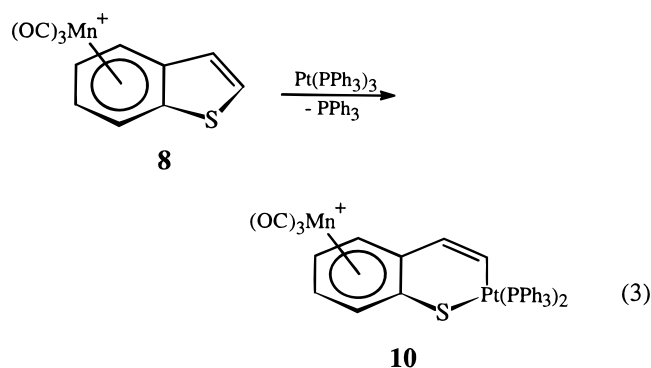
we demonstrated^{7a,8} that precoordination of Mn(CO)₃⁺ to the carbocyclic ring regioselectively activates the

system to reductive insertion of Mn(CO)₄ into the C(aryl)–S bond according to eq 2. (An analogous reac-



tion occurs with DBT.⁹) We reasoned that precoordination to the carbocyclic ring in **8** differentially weakens the C(aryl)–S bond over the C(2)–S bond, thus accounting for the reversal in regioselectivity compared to insertions with free BTs (which give **2**).

One may anticipate that the availability of multiple metal binding sites in a catalyst could provide for cooperativity in the key steps in HDS: C–S bond cleavage with metal insertion, hydrogenolysis of σ bonds, and desulfurization. Indeed, in homogeneous model studies, it is known^{2c,10} that multimetallic systems are superior to monometallic ones for the stoichiometric hydrodesulfurization of thiophenic molecules. The chemistry summarized by eq 2 established that the reactivity of the heterocyclic ring in BT can be significantly influenced by coordination of Mn(CO)₃⁺ to the carbocyclic ring. Ordinarily, complexation of the type shown in **8** electrophilically activates the arene ring to nucleophilic addition reactions, and indeed, common organic nucleophiles react with **8** in this manner to afford the expected cyclohexadienyl complexes.¹¹ Equation 2 differs from a nucleophilic addition reaction in that electrons, rather than a nucleophile, are being added, with the result that a metal fragment is transferred from one molecule into a C–S bond of another. This result prompted us to examine the *direct* reaction of **8** with a metal nucleophile. The nucleophile chosen, Pt(PPh₃)₃, does not react with free BT. It was found, however, that Pt(PPh₃)₃ reacts rapidly with **8** to give C–S insertion according to eq 3.



In this paper, we demonstrate that this activating effect is a general one. Thus, precoordination of any of the electrophilic metal fragments Ru(C₆Me₆)²⁺, Mn(CO)₃⁺, FeCp⁺, RuCp⁺, or Cr(CO)₃ to the π -system of T, BT, and DBT results in activation of a C–S bond

(5) (a) Rauchfuss, T. B. *Prog. Inorg. Chem.* **1991**, 39, 259. (b) Hockett, S. C.; Angelici, R. J. *Organometallics* **1988**, 7, 1491. (c) Choi, M.-G.; Angelici, R. J. *Organometallics* **1992**, 11, 3328. (d) Benson, J. W.; Angelici, R. J. *Organometallics* **1993**, 12, 680. (e) Angelici, R. J. *Bull. Soc. Chim. Belg.* **1995**, 104, 265. (f) Rudd, J. A.; Angelici, R. J. *Inorg. Chim. Acta* **1995**, 240, 393.

(6) Dailey, K. M. K.; Rauchfuss, T. B.; Rheingold, A. L.; Yap, G. P. A. *J. Am. Chem. Soc.* **1995**, 117, 6396.

(7) (a) Dullaghan, C. A.; Sun, S.; Carpenter, G. B.; Weldon, B.; Sweigart, D. A. *Angew. Chem.* **1996**, 108, 234; *Angew. Chem., Int. Ed. Engl.* **1996**, 35, 212. (b) Dullaghan, C. A.; Carpenter, G. B.; Sweigart, D. A.; Choi, D. S.; Lee, S. S.; Chung, Y. K. *Organometallics* **1997**, 16, 5688.

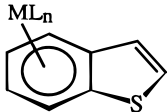
(8) (a) Zhang, X.; Dullaghan, C. A.; Watson, E. J.; Carpenter, G. B.; Sweigart, D. A. *Organometallics* **1998**, 17, 2067. (b) Sun, S.; Dullaghan, C. A.; Sweigart, D. A. *J. Chem. Soc., Dalton Trans.* **1996**, 4493. (c) Dullaghan, C. A.; Zhang, X.; Walther, D.; Carpenter, G. B.; Sweigart, D. A.; Meng, Q. *Organometallics* **1997**, 16, 5604.

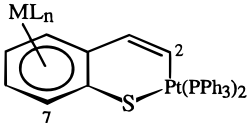
(9) Zhang, X.; Dullaghan, C. A.; Carpenter, G. B.; Sweigart, D. A.; Meng, Q. *J. Chem. Soc., Chem. Commun.* **1998**, 93.

(10) (a) Bianchini, C.; Meli, A. *J. Chem. Soc., Dalton Trans.* **1996**, 801. (b) Bianchini, C.; Jimenez, M. V.; Meli, A.; Moneti, S.; Patinec, V.; Vizza, F. *Organometallics* **1997**, 16, 5696.

(11) Lee, S. S.; Chung, Y. K.; Lee, S. W. *Inorg. Chim. Acta* **1996**, 253, 39.

Chart 1

	ML _n	label	ref.
	Mn(CO) ₃ ⁺	8	12
	FeCp ⁺	11	13
	RuCp ⁺	12	14
	Ru(C ₆ Me ₆) ²⁺	13	8a
	Cr(CO) ₃	14	15

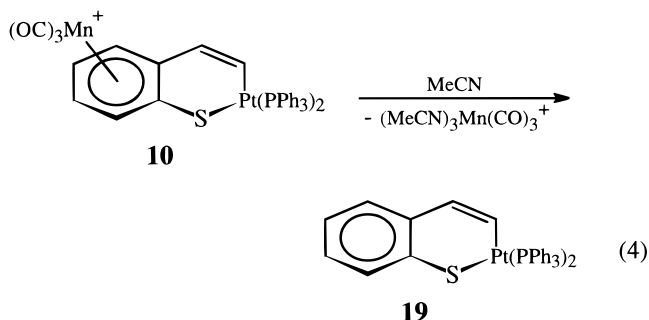
	ML _n	label
	Mn(CO) ₃ ⁺	10
	FeCp ⁺	15
	RuCp ⁺	16
	Ru(C ₆ Me ₆) ²⁺	17
	Cr(CO) ₃	18

to facile oxidative insertion by Pt(PPh₃)₃. It is suggested that this effect may be relevant to the chemistry occurring in heterogeneous HDS reactions.

Results and Discussion

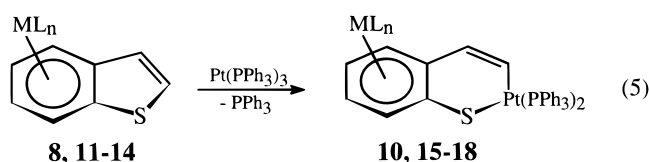
Benzothiophene Complexes. The known benzothiophene complexes depicted in Chart 1 were synthesized in order to study the effect of π -coordination on the ease of C–S bond cleavage and metal insertion upon addition of the nucleophilic reagent Pt(PPh₃)₃. As stated above, it is known⁴ that Pt(PET₃)₃ inserts reversibly into the C(2)–S bond of free BT to give **4**. By way of contrast, we found (as shown by ³¹P NMR) that Pt(PPh₃)₃ does not react with BT, even after refluxing for 12 h in CH₂Cl₂. Maitlis^{4a} noted previously that Pt(PPh₃)₃ does not react with free thiophenes under conditions that lead to insertion with Pt(PET₃)₃. That Pt(PPh₃)₃ is less nucleophilic than Pt(PET₃)₃ is, of course, not surprising. It has been shown, for example, that Pt(PET₃)₃ is ca. 1000 times more reactive than Pt(PPh₃)₃ toward the electrophile MeI.¹⁶

Although Pt(PPh₃)₃ is inert toward free BT, it was found to react rapidly with (η^6 -BT)Mn(CO)₃⁺ (**8**) at room-temperature according to eq 3 to afford the insertion product **10** in an isolated yield of 82%. IR spectra showed that under typical conditions the reaction has a half-life of less than 1 min. Derivatives of **10** bearing a 7-Et or a 2-Me substituent were synthesized by the same procedure. The platinum metallathiacycle **10**, as well as the analogues shown in Chart 1 (vide infra), are air stable but moderately light sensitive. Of the various metallathiacycles prepared, the derivative of **10** with a 2-Me substituent was found to be the least stable—probably due to unfavorable steric interactions (vide infra). The Mn(CO)₃⁺ moiety could be removed from **10** by refluxing for 1 h in MeCN, as shown in eq 4. This does not prove, however, whether the inability to



generate the simple metallathiacycle **19** from the reaction of free BT and Pt(PPh₃)₃ is due to a high kinetic barrier or due to thermodynamic instability.

The reaction of Pt(PPh₃)₃ with BT pre-coordinated to the fragments FeCp⁺, RuCp⁺, and Ru(C₆Me₆)²⁺ led cleanly to insertion products **15–17** (Chart 1; eq 5) in isolated yields of 76%, 80%, and 80%, respectively. With



(η^6 -BT)FeCp⁺ (**11**), an approximate half-life of 1 h at room temperature was estimated from ¹H NMR data in CD₂Cl₂. On the basis of the synthetic time scales and spectroscopic observations, the following qualitative order was found for the reactivity of the cationic BT complexes toward Pt(PPh₃)₃: Ru(C₆Me₆)²⁺, Mn(CO)₃⁺ > FeCp⁺, RuCp⁺. The mechanistic implications of this order are discussed below.

Verification of the proposed structures of the products of eq 5 was obtained from single-crystal X-ray diffraction studies of [**10**]BF₄ and [**15**]PF₆, Table 1. The cationic portions of these molecules are illustrated in Figures 1 and 2. The most significant feature of these structures is that the Pt(PPh₃)₂ moiety is inserted into the C(2)–S bond. Previously, we showed that Mn(CO)₄ inserts regioselectively into the C(aryl)–S bond in (η^6 -BT)Mn(CO)₃⁺, as in eq 2. A cursory examination of Figures 1 and 2 suggests that steric congestion would have been substantial had insertion into the C(aryl)–S bond occurred, although such a species cannot be ruled out as a reaction intermediate (vide infra). The metallathiacyclic ring in **10** is quite planar (mean deviation = 0.041 Å) and is nearly coplanar with the carbocyclic ring; the dihedral angle between these two planes is only 3.9°. The platinum atom in **10** adopts the usual square-planar geometry, although the P(1)–Pt(1)–P(2) angle is larger (96.5°) and the C(2)–Pt(1)–P(1) angle is smaller (85.2°) than the ideal angle of 90° due, presumably, to steric constraints imposed by the large phosphine ligands. Overall, the benzometallathiacycle portion of **10** is similar to that reported^{4a} by Maitlis for the Pt(PET₃)₂ insertion product of free BT (**4**).

Complex **15** (Figure 2) was found to crystallize with one molecule of well-ordered solvent (Et₂O). The platinum center in **15** is square planar, with much of the same angles as in **10**. There are, however, significant structural differences between these two complexes. Thus, the metallathiacyclic ring in **15** adopts a decidedly nonplanar conformation (mean deviation = 0.16 Å). The

(12) Sun, S.; Yeung, L. K.; Sweigart, D. A.; Lee, T.-Y.; Lee, S. S.; Chung, Y. K.; Switzer, S. R.; Pike, R. D. *Organometallics* **1995**, *14*, 2613.

(13) Lee, C. C.; Iqbal, M.; Gill, U. S.; Sutherland, R. G. *J. Organomet. Chem.* **1985**, *288*, 89.

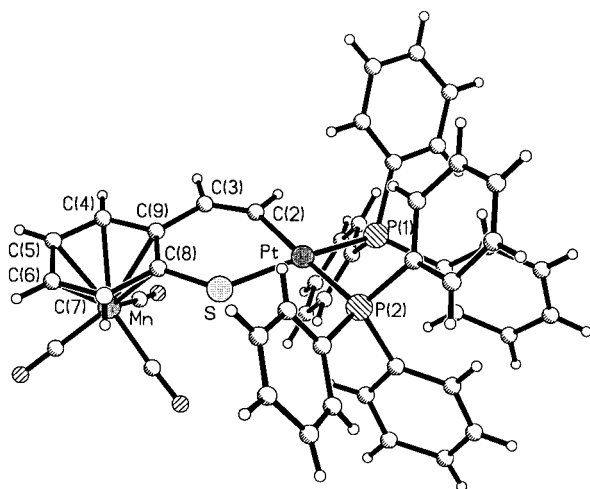
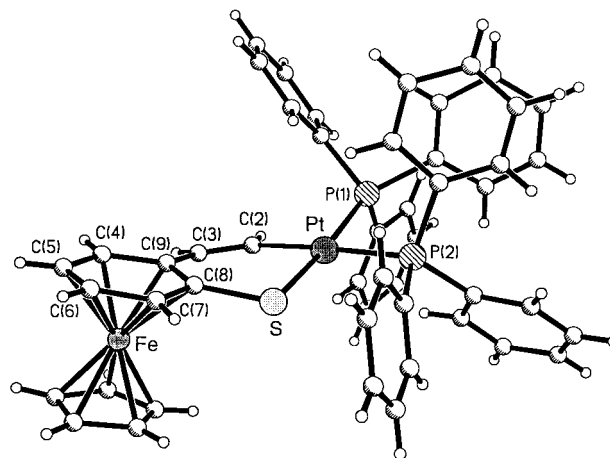
(14) Nolan, S. P.; Martin, K. L.; Stevens, E. D.; Fagan, P. J. *Organometallics* **1992**, *11*, 3947.

(15) Fischer, E. O.; Goodwin, H. A.; Kreiter, C. G.; Simmons, H. D.; Sonogashira, K.; Wild, S. B. *J. Organomet. Chem.* **1968**, *14*, 359.

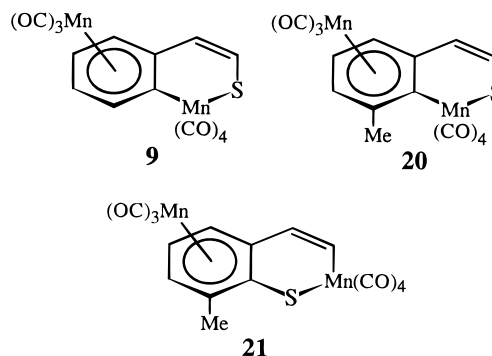
(16) Pearson, R. G.; Figdore, P. E. *J. Am. Chem. Soc.* **1980**, *102*, 1541.

Table 1. Crystallographic Data for Complexes **[10]BF₄** and **[15]PF₆**

	[10]BF₄	[15]PF₆·Et₂O
formula	C ₄₇ H ₃₆ BF ₄ MnO ₃ P ₂ PtS	C ₅₃ H ₅₁ F ₆ FeOP ₃ PtS
fw	1079.60	1193.85
temp, K	298	298
wavelength, Å	0.710 73	0.710 73
cryst syst	monoclinic	triclinic
space group	<i>P</i> 2 ₁ / <i>n</i>	<i>P</i> 1
<i>a</i> , Å	10.6371(3)	10.8906(2)
<i>b</i> , Å	30.6432(6)	15.2881(2)
<i>c</i> , Å	13.4551(3)	15.7410(2)
α, deg		75.2590(10)
β, deg	93.8890(10)	78.3060(10)
γ, deg		87.83
<i>V</i> , Å ³	4375.7(2)	2481.69(6)
<i>Z</i>	4	2
<i>d</i> _{calcd} , g cm ^{−3}	1.639	1.598
μ, mm ^{−1}	3.661	3.307
<i>F</i> (000)	2128	1192
cryst dims, mm	0.28 × 0.16 × 0.13	0.22 × 0.20 × 0.05
θ range, deg	1.33–23.25	1.68–26.53
no. of reflns collected	19 757	26 298
no. of indep reflns	6256 (<i>R</i> _{int} = 0.0946)	10091 (<i>R</i> _{int} = 0.0403)
data/restraints/params	6253/21/541	10091/27/595
GOF on <i>F</i> ²	1.049	1.042
final <i>R</i> indices [<i>I</i> > 2σ(<i>I</i>)]	<i>R</i> 1 = 0.0649, <i>wR</i> 2 = 0.1365	<i>R</i> 1 = 0.0410, <i>wR</i> 2 = 0.1019
<i>R</i> indices (all data)	<i>R</i> 1 = 0.1222, <i>wR</i> 2 = 0.1648	<i>R</i> 1 = 0.0529, <i>wR</i> 2 = 0.1084

**Figure 1.** Crystal structure of the cation in **[10]BF₄**. Selected bond distances (Å) and angles (deg) are Pt(1)–C(2) 2.052(14), C(2)–C(3) 1.26(2), C(3)–C(9) 1.47(2), C(9)–C(8) 1.37(2), C(8)–S(1) 1.75(2), Pt(1)–S(1) 2.279(4), Pt(1)–P(1) 2.297(3), Pt(1)–P(2) 2.346(3), C(2)–Pt(1)–S(1) 90.0(4), C(8)–S(1)–Pt(1) 113.4(5), C(3)–C(2)–Pt(1) 136.2(13), C(2)–Pt(1)–P(1) 85.2(4), P(1)–Pt(1)–P(2) 96.53(12), S(1)–Pt(1)–P(2) 88.81(13).**Figure 2.** Crystal structure of the cation in **[15]PF₆·Et₂O**. Selected bond distances (Å) and angles (deg) are Pt(1)–C(2) 2.056(5), C(2)–C(3) 1.287(8), C(3)–C(9) 1.456(9), C(9)–C(8) 1.423(9), C(8)–S(1) 1.775(6), Pt(1)–S(1) 2.2888(13), Pt(1)–P(1) 2.2952(12), Pt(1)–P(2) 2.3474(13), C(2)–Pt(1)–S(1) 89.65(16), C(8)–S(1)–Pt(1) 111.1(2), C(3)–C(2)–Pt(1) 133.9(5), C(2)–Pt(1)–P(1) 86.63(16), P(1)–Pt(1)–P(2) 96.69(4), S(1)–Pt(1)–P(2) 87.10(5).

situation is illustrated in Figure 3, which provides edge-on views of **10** and **15**. Experimental and theoretical¹⁷ studies suggest that the energy barrier(s) linking planar and various accessible nonplanar conformations in thiophenic metallathiacycles can be low and that steric factors play a dominant role in this regard. An illustration of this point is provided by complexes **9**, **20**, and **21**. The first two of these complexes have highly nonplanar metallathiacyclic rings, while the third adopts a planar conformation.^{8c} It is most probable that steric factors are important in **9** and **20** but not in **21**. The influence of steric effects is further indicated by the fact that **20** has a very different nonplanar conformation



from that in **9** as a result of the methyl substituent. In the case of **15**, the observed nonplanarity could result from modest steric interaction between a PPh₃ ligand

(17) Blonski, C.; Myers, A. W.; Palmer, M.; Harris, S.; Jones, W. D. *Organometallics* **1997**, *16*, 3819.

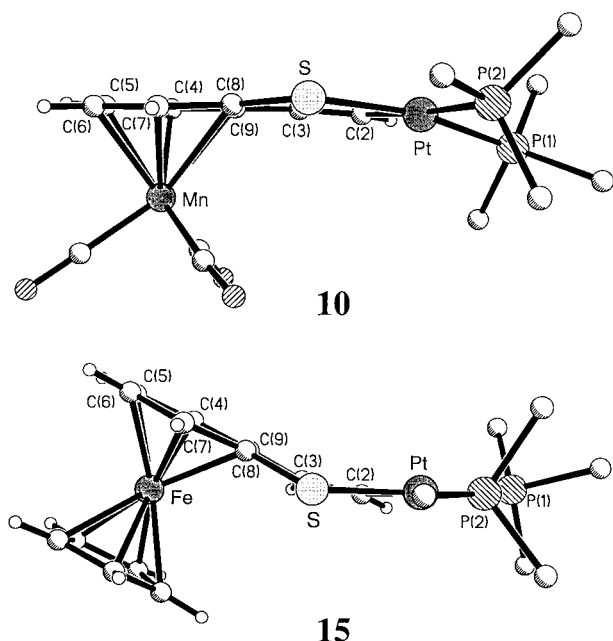


Figure 3. Edge-on views of insertion products **10** and **15**. For clarity, only the phenyl ring carbon atoms directly bonded to the phosphorus atoms are shown.

and the Cp ring or could be the result of solid-state packing.

In contrast to the insertion of $\text{Pt}(\text{PPh}_3)_3$ into BT complexes containing cationic metal fragments (**8**, **11**–**13**), the reaction with $(\eta^6\text{-BT})\text{Cr}(\text{CO})_3$ (**14**) took place much more slowly and required heating. The reaction in refluxing CH_2Cl_2 with 1.6 equiv of $\text{Pt}(\text{PPh}_3)_3$ to give the insertion product **18** occurred with a half-life of ca. 3 h and was terminated after approximately 75% completion due to the onset of decomposition. In the presence of 3 equiv of PPh_3 , the rate was greatly retarded, with the half-life increasing to ca. 30 h (after which the reaction was discontinued). Evidence was obtained that the insertion of $\text{Pt}(\text{PPh}_3)_3$ into **14** is a reversible process, in analogy to that reported^{4a} for **4**. Thus, refluxing **18** in CH_2Cl_2 for 20 h with 7.6 equiv of PPh_3 resulted in ca. 20% deinsertion to produce **14**; it was not determined if the reaction had reached equilibrium.

Mechanism of Insertion into Benzothiophene Complexes. The experimental data show that the relative rate of $\text{Pt}(\text{PPh}_3)_3$ insertion into BT complexes according to eq 5 depends on the ML_n fragment as follows: $\text{Ru}(\text{C}_6\text{Me}_6)^{2+}$, $\text{Mn}(\text{CO})_3^+ > \text{FeCp}^+$, $\text{RuCp}^+ \gg \text{Cr}(\text{CO})_3$. On the basis of extensive studies,¹⁸ it is expected that coordination of the ML_n fragment to BT should electrophilically activate the carbocyclic ring to attack by nucleophiles in the order indicated above. For example, $\text{Mn}(\text{CO})_3^+$ is predicted to be 10^4 times more activating than FeCp^+ . However, the reaction in question, eq 5, does not involve nucleophilic attack on the carbocyclic ring but rather insertion into the olefinic C(2)–S bond of the heterocyclic ring. Nevertheless, the data indicate that the same qualitative reactivity order prevails for eq 5. The ML_n moieties in **8** and **11**–**14** function to activate a C–S bond to nucleophilic cleavage

by $\text{Pt}(\text{PPh}_3)_3$. A plausible mechanism involves initial η^1 coordination of $\text{Pt}(\text{PPh}_3)_3$ to the sulfur atom, followed by insertion of the platinum into a C–S bond (which can also be viewed as oxidative addition of a C–S group to Pt). At some point along the reaction pathway, a PPh_3 ligand is lost, most likely prior to or in concert with the actual insertion. In accordance with this, the reaction of $\text{Pt}(\text{PPh}_3)_3$ with **14** was found to be significantly inhibited by the presence of excess PPh_3 (vide supra).

Although the details of the mechanism of eq 5 are unknown, it is apparent that initial formation of an η^1 -S intermediate cannot be the rate-determining step. This follows from the observation that the most electron-withdrawing ML_n fragments are the most activating, which would not be expected if the rate-determining step were coordination of the sulfur atom to $\text{Pt}(\text{PPh}_3)_n$. It was noted above that insertion of $\text{Mn}(\text{CO})_4$ into **8** occurs regiospecifically at the C(aryl)–S bond (eq 2). In contrast, $\text{Pt}(\text{PPh}_3)_3$ inserts regiospecifically into the C(2)–S bond in **8** and **11**–**14** (eq 5), most likely because of steric effects. We are of the opinion that precoordination of ML_n to BT selectively weakens that C(aryl)–S bond, and it is possible that C(aryl)–S cleavage is favored kinetically in eq 5 to afford an intermediate that isomerizes to the thermodynamically preferred C(2)–Pt–S product. Such an isomerization with a $\text{Mn}(\text{CO})_4$ fragment has been shown^{8c} to be facile at room temperature in the conversion of **20** to **21**. In addition, it is shown below that $\text{Pt}(\text{PPh}_3)_3$ inserts into $(\eta^6\text{-DBT})\text{Mn}(\text{CO})_3^+$, which necessarily involves cleavage of a C(aryl)–S bond (albeit at the one farther away from the $\text{Mn}(\text{CO})_3$ group). Possibly related to this is the observation that $(\eta^6\text{-2-MeBT})\text{Mn}(\text{CO})_3^+$ reacted with $\text{Pt}(\text{PPh}_3)_3$ to give a product that could be isolated but was thermally unstable in comparison to the insertion product (**10**) with $(\eta^6\text{-BT})\text{Mn}(\text{CO})_3^+$ (**8**) while reaction of $(\eta^6\text{-2,7-Me}_2\text{BT})\text{Mn}(\text{CO})_3^+$ with $\text{Pt}(\text{PPh}_3)_3$ gave a product that could not be isolated. NMR, IR, MS, and elemental analysis data clearly indicate that $(\eta^6\text{-2-MeBT})\text{Mn}(\text{CO})_3^+$ reacts with $\text{Pt}(\text{PPh}_3)_3$ to insert $\text{Pt}(\text{PPh}_3)_2$ into a C–S bond, but we cannot prove which C–S bond is cleaved. However, consideration of ^{31}P NMR data (see Experimental Section) show that complexes **10** and **15**–**18** all have very similar δ and $J_{\text{Pt-P}}$ values. The ^{31}P NMR parameters of the insertion product with $(\eta^6\text{-2-MeBT})\text{Mn}(\text{CO})_3^+$ are noticeably different and, in fact, are close to those found for the insertion product obtained from $(\eta^6\text{-DBT})\text{Mn}(\text{CO})_3^+$, which must contain a C(aryl)–Pt–S link. Thus, we believe that the 2-methyl group in $(\eta^6\text{-2-MeBT})\text{Mn}(\text{CO})_3^+$ forces insertion to occur at the C(aryl)–S bond. Significantly, this suggestion accounts for the inability to isolate an insertion product with $(\eta^6\text{-2,7-Me}_2\text{BT})\text{Mn}(\text{CO})_3^+$.

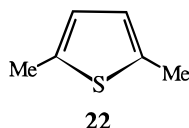
Of relevance to the present paper is a recent study by Angelici and co-workers^{5f} on the ability of the $\text{CpRe}(\text{CO})_2$ fragment to coordinate to the sulfur and to the C(2)=C(3) double bond in benzothiophenes. In comparison to results with free BT, it was found that η^6 -coordination of the $\text{Cr}(\text{CO})_3$ group promotes $\text{CpRe}(\text{CO})_2$ binding to the double bond. This led to the suggestion that η^6 adsorption of BT on a metal site in a HDS catalyst should promote coordination of the double bond

(18) (a) Kane-Maguire, L. A. P.; Honig, E. D.; Sweigart, D. A. *Chem. Rev.* **1984**, *84*, 525. (b) Pike, R. D.; Sweigart, D. A. *Synlett* **1990**, 565.

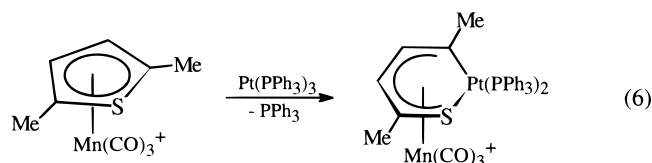
to another metal site. In this manner, hydrogenation of the C(2)=C(3) bond would be facilitated, as proposed to occur in an initial step of a major HDS pathway for BT. In view of our results with complexes **8** and **11–14**, it is suggested that η^6 adsorption of BT also promotes C–S bond cleavage, which is a prelude to desulfurization (and hydrogenolysis) in HDS chemistry.

Thiophene and Dibenzothiophene Complexes.

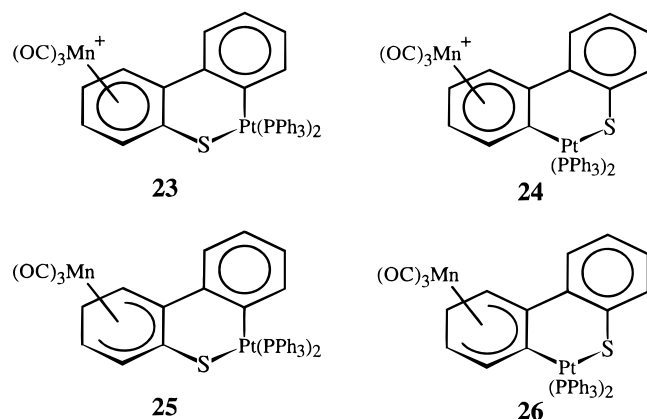
Insertion of a variety of metal fragments into a C–S bond in free thiophene (T) has been reported.^{2–4} Pt(PET₃)₃ was shown⁴ to insert into T, 2-MeT, and 3-MeT to afford derivatives of **3**, but no reaction was observed with the sterically encumbered thiophene 2,5-Me₂T (**22**).



We found that Pt(PPh₃)₃ is unreactive toward free T but readily inserts when the π -system is precoordinates to Mn(CO)₃⁺. The activating effect of Mn(CO)₃⁺ is dramatically illustrated with 2,5-Me₂T, which reacts rapidly at room temperature according to eq 6.



Pt(PPh₃)₃ also inserts rapidly into (η^6 -DBT)Mn(CO)₃⁺ to afford **23**. The alternative structure **24** was judged



unlikely based on steric considerations and on a comparison of ³¹P NMR data of the product with that of the cyclohexadienyl complex obtained after hydride addition to the coordinated arene ring (**25**, **26**). The ³¹P NMR chemical shifts on average changed by only 0.74 ppm, which is more consistent with the transformation **23** → **25** than with **24** → **26**. In a control experiment, hydride addition to the arene ring in the BT complex **10** was found to change the ³¹P NMR chemical shifts by an average of 1.7 ppm.

Conclusions

Coordination of any of a variety of transition-metal fragments to the π -system of thiophene, benzothiophene, and dibenzothiophene results in activation of a C–S

bond to rapid insertion by the weak nucleophile Pt(PPh₃)₃. Cleavage of a C–S bond via metal insertion is a key step in HDS chemistry, and the results presented herein suggest that π -adsorption of the thiophenic substrate on the catalyst surface may facilitate this process, as well as subsequent desulfurization and hydrogenolysis.

Experimental Section

Materials. Standard reagents were purchased from commercial sources and used without further purification. The following compounds were synthesized by the indicated literature method: [η^6 -R-BT)Mn(CO)₃]BF₄ (R = H, 2-Me, 7-Et),¹² [η^5 -2,5-Me₂T)Mn(CO)₃]BF₄,¹⁹ (η^6 -BT)Cr(CO)₃,¹⁵ [η^6 -BT)FeCp]PF₆,¹³ [η^6 -BT)RuCp]PF₆,¹⁴ [η^6 -BT)Ru(C₆Me₆)]BF₄,^{8a} [η^6 -DBT)Mn(CO)₃]BF₄,¹² and Pt(PPh₃)₃.²⁰ Activated neutral alumina (Brockmann I, 150 mesh) was deactivated by adding water to form a 10% w/w mixture. ³¹P NMR chemical shifts are relative to a 85% phosphoric acid external reference.

Crystal Structure Determinations. The crystal structures of [**10**]BF₄ and [**15**]PF₆·Et₂O were determined with a Siemens P4 diffractometer equipped with a CCD area detector and controlled by SMART version 4 software. Data reduction was carried out by SAINT version 4 and included profile analysis; this was followed by absorption correction using the program SADABS. Data were collected at 25 °C with Mo K α radiation. The structures were determined by direct methods and refined on *F*² using the SHELXTL version 5 package. Hydrogen atoms were introduced in ideal positions, riding on the carbon atom to which they are bonded; each was refined with isotropic temperature factors ranging from 20% to 50% greater than that of the ridden atom. All other atoms were refined with anisotropic thermal parameters.

Insertion of Pt(PPh₃)₃ into (η^6 -BT)Mn(CO)₃⁺ (8**).** Pt(PPh₃)₃ (0.300 g, 0.305 mmol) was added to a suspension of [η^6 -BT)Mn(CO)₃]BF₄ (0.120 g, 0.30 mmol) in CH₂Cl₂ (8 mL) under N₂ at room temperature. An immediate color change from bright yellow to orange occurred. After 15 min, the volume was reduced to 3 mL and the product precipitated by addition of Et₂O. Reprecipitation from acetone with Et₂O afforded pure [**10**]BF₄ as a yellow powder. [**10**]BF₄: yield 82% (0.279 g). IR (acetone): ν_{CO} 2058 (s), 2000 (s, br) cm⁻¹. ¹H NMR (CD₃C(O)CD₃): δ 7.52–7.05 (m, 32H, Ph, H₂, 3), 6.94 (br, 1H), 6.71 (br, 1H), 6.60 (br, 1H), 5.29 (br, 1H). ³¹P NMR (CD₃C(O)CD₃): δ 26.49 (dd, *J*_{P–P} = 22 Hz, *J*_{P–Pt} = 3414 Hz), 22.15 (dd, *J*_{P–P} = 22 Hz, *J*_{P–Pt} = 1900 Hz). ³¹P NMR (CD₂-Cl₂): δ 26.04 (dd, *J*_{P–P} = 23 Hz, *J*_{P–Pt} = 3428 Hz), 21.75 (dd, *J*_{P–P} = 23 Hz, *J*_{P–Pt} = 1901 Hz). MS FAB: 992 (M⁺ – BF₄[–]), 730 (M⁺ – PPh₃). Anal. Calcd for C₄₇H₃₆O₃MnPtS₂BF₄: C, 52.29; H, 3.36. Found: C, 52.03; H, 3.44. A crystal of [**10**]BF₄ suitable for X-ray diffraction was grown by vapor diffusion of Et₂O into an acetone solution of the complex at –15 °C over a period of several days.

The Mn(CO)₃⁺ was removed from **10** according to eq 4 by dissolving [**10**]BF₄ (0.065 g, 0.060 mmol) in CH₃CN (10 mL) and heating to reflux under N₂ for 1 h. After this time, an IR spectrum showed complete conversion of the manganese to (MeCN)₃Mn(CO)₃⁺. The solvent was removed in vacuo, and the residue was redissolved in CH₂Cl₂, loaded onto a dry activated alumina column, and eluted with acetone. The solvent was removed, and the oily residue of **19** was washed with hexanes. For **19**: yield 60% (0.030 g). ¹H NMR (CD₂-

(19) (a) Lesch, D. A.; Richardson, J. W.; Jacobson, R. A.; Angelici, R. J. *J. Am. Chem. Soc.* **1984**, *106*, 2901. (b) Chen, J.; Young, V. G.; Angelici, R. J. *Organometallics* **1996**, *15*, 325. (c) Lee, S. S.; Lee, T. Y.; Choi, D. S.; Lee, J. S.; Chung, Y. K.; Lee, S. W.; Lah, M. S. *Organometallics* **1997**, *16*, 1749.

(20) Yoshida, T.; Matsuda, T.; Otsuka, S. *Inorg. Synth.* **1990**, *28*, 123.

Cl₂): δ 7.86 (m, 1H), 7.71–6.80 (m, 35H). ³¹P NMR (CD₂Cl₂): δ 28.07 (dd, J_{P-P} = 21.5 Hz, J_{P-Pt} = 3246 Hz), 26.18 (dd, J_{P-P} = 21.5 Hz, J_{P-Pt} = 1852 Hz).

Insertion of Pt(PPh₃)₃ into (η^6 -R-BT)Mn(CO)₃⁺ (R = 2-Me, 7-Et) was performed similarly to the method described above for the synthesis of [10]BF₄. [η^6 -2-MeBT-Pt(PPh₃)₂]Mn(CO)₃·BF₄: yield 89% (0.160 g). IR (CH₂Cl₂): ν_{CO} 2056 (s), 2002 (s), 1992 (s) cm⁻¹. ¹H NMR (CD₃C(O)CD₃): δ 7.80–7.05 (m, 30H, Ph), 6.57 (m, 1H), 6.43 (m, 1H), 6.24 (m, 1H), 6.15 (m, 1H), 5.37 (m, 1H), 2.21 (s, Me). ³¹P NMR (CD₃C(O)CD₃): δ 25.81 (dd, J_{P-P} = 21 Hz, J_{P-Pt} = 3156 Hz), 16.03 (dd, J_{P-P} = 21 Hz, J_{P-Pt} = 2074 Hz). HR MS: M⁺ (m/z) calcd 1006.1045, obsd 1006.1023. Anal. Calcd for C₄₈H₃₈O₃MnP₂PtSbF₄: C, 52.72; H, 3.50. Found: C, 52.71; H, 3.74. For [η^6 -7-EtBT-Pt(PPh₃)₂]Mn(CO)₃·BF₄: yield 90% (0.090 g). IR (CH₂Cl₂): ν_{CO} 2056 (s), 1996 (s, br) cm⁻¹. ¹H NMR (CD₃C(O)CD₃): δ 7.84–7.10 (m, 32H, Ph, H₂, 3), 6.82 (m, H₄, 7), 6.56 (m, H₆), 6.41 (m, H₅), 2.62 (m, CH₂), 1.09 (t, J = 7.1 Hz, Me). ³¹P NMR (CD₃C(O)CD₃): δ 26.55 (dd, J_{P-P} = 21 Hz, J_{P-Pt} = 3418 Hz), 24.11 (dd, J_{P-P} = 21 Hz, J_{P-Pt} = 1916 Hz). Anal. Calcd for C₄₉H₄₀O₃MnP₂PtSbF₄: C, 53.13; H, 3.64. Found: C, 53.03; H, 3.47.

Insertion of Pt(PPh₃)₃ into (η^6 -BT)FeCp⁺ (11). Pt(PPh₃)₃ (0.050 g, 0.055 mmol) was added to a solution of [η^6 -BT)FeCp]PF₆ (0.020 g, 0.050 mmol) in CH₂Cl₂ (5 mL) under N₂ at room temperature. The color changed from bright yellow to orange-red and ultimately to orange. After 2 h, the solvent was removed in vacuo and the orange residue of [15]PF₆ was recrystallized from CH₂Cl₂/Et₂O. [15]PF₆: yield 76% (0.043 g). ¹H NMR (CD₂Cl₂): δ 7.57–7.30 (m, 18H, Ph), 7.30–7.10 (m, 13H, Ph, H₂), 6.68 (br, H₃), 6.34 (br, H₅ or H₆), 6.16 (br, H₅ or H₆), 5.81 (m, 2H, H₄, 7), 4.50 (s, 5H, Cp). ³¹P NMR (CD₂Cl₂): δ 25.48 (dd, J_{P-P} = 22 Hz, J_{P-Pt} = 3350 Hz), 21.91 (dd, J_{P-P} = 21.5 Hz, J_{P-Pt} = 1880 Hz), –143.97 (sept, J_{P-F} = 709 Hz). Anal. Calcd for C₄₉H₄₁FeP₃PtSF₆: C, 52.56; H, 3.69. Found: C, 52.45; H, 3.84. A crystal of [15]PF₆·Et₂O suitable for X-ray diffraction was grown by vapor diffusion of Et₂O into an acetone solution of the complex at –15 °C over a period of several days.

Insertion of Pt(PPh₃)₃ into (η^6 -BT)RuCp⁺ (12) and (η^6 -BT)Ru(C₆Me₆)²⁺ (13). The procedure followed for these reactions is essentially the same as that described above for 11, with reaction times being 2 h for 12 and 20 min for 13. [16]PF₆: yield 80% (0.114 g). ¹H NMR (CD₂Cl₂): δ 7.43–7.30 (m, 18H, Ph), 7.30–7.15 (m, 13H, Ph, H₂), 6.50 (m, H₃), 6.41 (m, H₅ or H₆), 6.02 (m, H₅ or H₆), 5.76 (m, 2H, H₄, 7), 4.92 (s, 5H, Cp). ³¹P NMR (CD₂Cl₂): δ 26.46 (dd, J_{P-P} = 22 Hz, J_{P-Pt} = 3350 Hz), 22.47 (dd, J_{P-P} = 21.5 Hz, J_{P-Pt} = 1880 Hz). HR MS: M⁺ (m/z) calcd 1020.1095, obsd 1020.1081. Anal. Calcd for C₄₉H₄₁RuP₃PtSF₆: C, 50.47; H, 3.55. Found: C, 50.52; H, 3.55. For [17][BF₄]₂: yield 80% (0.135 g). ¹H NMR (CD₂Cl₂): δ 8.11 (m, H₂), 7.49–7.21 (m, 30H, Ph), 6.43 (t, J = 5.7 Hz, H₆), 6.36 (t, J = 5.7 Hz, H₅), 6.27 (d, J = 6.0 Hz, H₇), 6.22 (m, H₃), 6.07 (d, J = 5.8 Hz, H₄), 2.14 (s, C₆Me₆). ³¹P NMR (CD₂Cl₂): δ 25.29 (dd, J_{P-P} = 24 Hz, J_{P-Pt} = 3446 Hz), 21.26

(dd, J_{P-P} = 24 Hz, J_{P-Pt} = 1921 Hz). Anal. Calcd for C₅₆H₅₄·RuP₂PtSbF₈: C, 52.11; H, 4.22. Found: C, 51.83; H, 4.29.

Insertion of Pt(PPh₃)₃ into (η^6 -BT)Cr(CO)₃ (14). A solution of (η^6 -BT)Cr(CO)₃ (0.022 g, 0.081 mmol) in CH₂Cl₂ (20 mL) under N₂ was warmed to reflux, and Pt(PPh₃)₃ (0.130 g, 0.132 mmol) was then added. After the mixture was refluxed for 10 h, the solution was concentrated to 3 mL and loaded onto a deactivated alumina column. Hexanes was used to elute impurities and then Et₂O/hexanes (1:2) to elute (BT)Cr(CO)₃ (0.005 g). The product (18) was finally eluted with Et₂O/hexanes (3:1) and obtained as a yellow solid after drying. 18: yield 84% (0.052 g) based on the amount of 14 consumed. IR (CH₂Cl₂): ν_{CO} 1946 (s), 1868 (s, br) cm⁻¹. IR (hexanes): ν_{CO} 1952 (s), 1881 (s, br) cm⁻¹. ¹H NMR (CD₂Cl₂): δ 7.80–7.14 (m, 30H, Ph), 7.06 (m, H₂), 6.50 (m, H₃), 5.79 (d, J = 6.7, H₇), 5.65 (dd, J = 1.2, 6.6 Hz, H₄), 5.38 (dt, J = 1.3, 6.4 Hz, H₆), 5.05 (dt, J = 1.2, 6.3 Hz, H₅). ³¹P NMR (CD₃C(O)CD₃): δ 26.95 (dd, J_{P-P} = 21 Hz, J_{P-Pt} = 3348 Hz), 23.33 (dd, J_{P-P} = 21 Hz, J_{P-Pt} = 1874 Hz). Anal. Calcd for C₄₇H₃₆O₃CrP₂PtS: C, 57.03; H, 3.67. Found: C, 57.38; H, 4.06.

Insertion of Pt(PPh₃)₃ into (η^5 -2,5-Me₂T)Mn(CO)₃⁺ and (η^6 -DBT)Mn(CO)₃⁺. The procedure followed for these reactions is essentially the same as that described above for 11, with the reaction time being 15 min in both cases. [η^5 -2,5-Me₂T·Pt(PPh₃)₂]Mn(CO)₃·BF₄ (see eq 6): yield 80% (0.112 g). IR (CH₂Cl₂): ν_{CO} 2039 (s), 1977 (s), 1966 (s) cm⁻¹. ¹H NMR (CD₃C(O)CD₃): δ 7.60–7.15 (m, 30H, Ph), 6.90 (m, 1H), 4.68 (m, 1H), 2.41 (s, Me), 1.57 (m, Me). ³¹P NMR (CD₃C(O)CD₃): δ 19.57 (dd, J_{P-P} = 20.5 Hz, J_{P-Pt} = 1984 Hz), 16.42 (dd, J_{P-P} = 20.5 Hz, J_{P-Pt} = 3638 Hz). HR MS: M⁺ (m/z) calcd 970.1046, obsd 970.1019. Anal. Calcd for C₄₅H₃₈O₃MnP₂PtSbF₄: C, 51.08; H, 3.62. Found: C, 51.32; H, 3.52. [η^6 -DBT·Pt(PPh₃)₂]Mn(CO)₃·BF₄ ([23]BF₄): yield 88% (0.180 g). IR (CH₂Cl₂): ν_{CO} 2058 (s), 2006 (s), 1996 (s) cm⁻¹. ¹H NMR (CD₂Cl₂): δ 7.58 (d, J = 7.2 Hz, 1H), 7.50–7.20 (m, 33H, Ph), 6.32 (1H), 6.18 (1H), 5.92 (1H), 5.30 (1H). ³¹P NMR (CD₂Cl₂): δ 24.64 (dd, J_{P-P} = 20 Hz, J_{P-Pt} = 3116 Hz), 15.75 (dd, J_{P-P} = 19.5 Hz, J_{P-Pt} = 2110 Hz). MS FAB: 1042 (M⁺). Anal. Calcd for C₅₁H₃₈O₃MnP₂PtSbF₄: C, 54.22; H, 3.39. Found: C, 53.59; H, 3.62.

Acknowledgment. This work was supported by grants from the National Science Foundation (Grant No. CHE-9705121) and the Petroleum Research Fund, administered by the American Chemical Society.

Supporting Information Available: Tables of atomic coordinates, bond lengths and angles, anisotropic displacement parameters, and hydrogen coordinates for [10]BF₄ and [15]PF₆·Et₂O (49 pages). Ordering information is given on any current masthead page.

OM9802865